Variation of Bragg condition in low-glass-transition photorefractive polymers when recorded in reflection geometry

M. Eralp[1], J. Thomas[1], S. Tay[1], P.-A. Blanche[1], A. Schülzgen[1], R. A. Norwood[1], M. Yamamoto[2], and N. Peyghambarian[1]

[1]College of Optical Sciences, The University of Arizona, Tucson, AZ 85721
Tel: (520) 621 8227; fax: (520) 626 6219; muhsin@optics.arizona.edu
[2]Nitto Denko Technical, 401 Jones Rd., Oceanside CA 92054

Abstract: Two low-glass transition photorefractive polymer composites were investigated in a symmetric reflection geometry. The holograms recorded in 105 μm thick devices have reached diffraction efficiencies as high as 60%. Unlike the gratings recorded in transmission geometry, holograms recorded in reflection geometry showed high angular selectivity and the Bragg condition was observed to be sensitive to the magnitude of the external bias field. We attribute this effect to poling-induced birefringence and give a theoretical analysis to describe the observed results.

OCIS codes: (050.7330) Volume gratings, (190.5330) Photorefractive optics

References and links

1. D. Psaltis and F. Mok, "Holographic memories," Sci. Am. **273**, 70–76 (1995).
2. S. Wu, Q. Song, A. Mayers, D. A. Gregory, and F. T. S. Yu, "Reconfigurable interconnections using photorefractive holograms," Appl. Opt. **29**, 1118-1125 (1990).
3. R. T. B. James, C. Wah, K. Iizuka, and H. Shimotahira, "Optically tunable optical filter," Appl. Opt. **34,** 8230 (1995).
4. G. Li, M. Eralp, J. Thomas, S. Tay, A. Schülzgen, R. A. Norwood, and N. Peyghambarian, "All-optical dynamic correction of distorted communication signals using a photorefractive polymeric hologram," Appl. Phys. Lett. **86**, 161103 (2005).
5. B. Kippelen and N. Peyghambarian, in *Polymers for Photonic Applications II*, (Springer-Verlag: Berlin, 2003) Vol. **161**, Chap. 2.
6. K. Meerholz, B. L. Volodin, B. K. Sandalphon, and N. Peyghambarian, "Peptide oligomers for holographic data storage," Nature **371**, 497-500 (1994).
7. D. Wright, M. A. Diaz-Garcia, J. D. Casperson, M. DeClue, W. E. Moerner, and R. J. Twieg, "High-speed photorefractive polymer composites," Appl. Phys. Lett. **73**, 1490 (1998).
8. J. A. Herlocker, K. B. Ferrio, E. Hendrickx, B. D. Guenther, S. Mery, B. Kippelen, and N. Peyghambarian, "Direct observation of orientation limit in a fast photorefractive polymer composite," Appl. Phys. Lett. **74**, 2253 (1999).
9. M. Eralp, J. Thomas, S. Tay, G. Li, G. Meredith, A. Schülzgen, G. A. Walker, S. Barlow, S. R. Marder, and N. Peyghambarian, "High-performance photorefractive polymer operating at 975 nm," Appl. Phys. Lett. **85**, 1095 (2004).
10. S. Tay, J. Thomas, M. Eralp, G. Li, S. Marder, G. A. Walker, S. Barlow, M. Yamamoto, R. Norwood, A. Schülzgen, and N. Peyghambarian, "High-performance photorefractive polymer operating at 1550 nm with near-video-rate response time," Appl. Phys. Lett **87**, 171105 (2005).
11. O-P. Kwon, G. Montemezzani, P. Günter, and S-H. Lee, "High-gain photorefractive reflection gratings in layered photoconductive polymers," Appl. Phys. Lett. **84**, 43-45 (2004).
12. F. Gallego-Gomez, M. Salvador, S. Köber, and K. Meerholz, "High-performance reflection gratings in photorefractive polymers," Appl. Phys. Lett **90**, 251113 1-3 (2007)
13. W. E. Moerner, S. M. Silence, F. Hache, and G. C. Bjorklund, "Orientationally enhanced photorefractive effect in polymers," J. Opt. Soc. Am. B **11**, 320 (1994).
14. J. Thomas, C. Fuentes-Hernandez, M. Yamamoto, K. Cammack, K. Matsumoto, G. Walker, S. Barlow, G. Meredith, B. Kippelen, S. R. Marder, and N. Peyghambarian, "High-performance photorefractive polymer operating at 1550 nm with near-video-rate response time," Adv. Mater. **16**, 2032 (2004).

#84805 - $15.00 USD Received 6 Jul 2007; revised 22 Aug 2007; accepted 22 Aug 2007; published 28 Aug 2007

15. E. Hendrickx, Y. D. Zhang, K. B. Ferrio, J. A. Herlocker, J. Anderson, N. R. Armstrong, E. A. Mash, A. P. Persoons, N. Peyghambarian, and B. Kippelen, J. Mater. Chem. **9**, 2251 (1999).
16. N. V. Kuktharev, V. B. Markov, S. G. Odulov, M. S. Soskin, and V. L. Vinetskii, "Holographic storage in electrooptic crystals," Ferroelectrics **22**, 949 (1979).
17. C. Fuentes-Hernandez, J. Thomas, R. Termine, G. Meredith, S. Barlow, G. Walker, K. Cammack, K. Matsumoto, M. Yamamoto, S. R. Marder, B. Kippelen, and N. Peyghambarian, "Video-rate compatible photorefractive polymers with stable dynamic properties under continuous operation," Appl. Phys. Lett. **85**, 1877 (2004).
18. W.-J. Joo, H. Chun, I. K. Moon, and N. Kim, "Dependence of the Bragg condition on an external electric field for a Polymeric Photorefractive Material," Appl. Opt. **42**, 3271 (2003).
19. D. M. Burland, R. D. Miller, and C. A. Walsh, "Second-order nonlinearity in poled-polymer systems," Chem. Rev. **94**, 31 (1994).
20. H. Kogelnik, "Coupled-wave theory for thick hologram gratings," Bell Syst. Tech. J. **48**, 2909 (1969).

1. Introduction

Photorefractive (PR) materials have been investigated for many applications such as dynamic holographic memories [1], reconfigurable interconnects [2], tunable filters [3] and beam cleanup [4]. PR polymer composites have gained attention due to their low-cost and the tunability of their properties, as well as their large optical nonlinearity compared to their inorganic counterparts [5]. Thin film devices of these polymer composites have shown 100% diffraction efficiencies [6], millisecond response times [7, 8] and sensitivity in the infrared [9, 10]. Almost all of these research accomplishments were conducted in the slanted transmission geometry due to the large efficiencies obtained with this particular geometry. However, for some applications the alternative reflection geometry can be more attractive, especially when the reconstructing light is desired to be on the viewer's side and in cases where a white light source is preferred for reconstruction. In recent publications, PR polymers were studied in the reflection geometry but the measured diffraction efficiency was low [11, 12]. Because of the many potential applications of the reflection geometry, we have studied two PR polymer composites in reflection geometry and analyzed the unusual behavior observed in the measurements.

In the standard transmission geometry, a slant angle between the sample normal and writing beams' bisector is necessary since (1) the effective electro-optic coefficient will be non-zero due to the uniaxial symmetry of poled polymers and (2) there will be a component of the electric field along the grating wave vector, K, providing a drift source for carriers. Indeed, in polymer composites, an external electric field is necessary to dissociate charges, transport carriers and orient polar molecules (chromophores) that provide a refractive index change. The magnitude of the external field projection on K depends on the slant angle. On the other hand, in the reflection geometry, the bias field has a larger projection along the grating vector for a wide range of writing angles. So, the introduction of a slant angle is not required.

In a polymer with its glass-transition temperature near the operating temperature, the chromophores, which are necessary constituents of a PR polymer composite, can be aligned not only by the external electric field but also by the sinusoidally varying space-charge field during grating formation. The orientational enhancement effect [13] brings the advantage of higher diffraction efficiencies and gain coefficients. However, it also introduces a field-dependent birefringence. The alignment of the chromophore along the applied field causes a change in the index ellipsoid of the sample, which consequently influences the Bragg condition.

2. Experiment

The two composites we studied were based on the hole-transport polymers PATPD [14] and poly(*N*-vinylcarbazole) (PVK) which were doped with nonlinear optical chromophores (DBDC [14] and 7-DCST [15]), the plasticizer *N*-ethyl carbazole (ECZ) or butyl benzyl phthalate (BBP), and C_{60} as a sensitizer for charge generation at an operating wavelength of 633nm. Composites prepared included PATPD/DBDC/ECZ/C_{60} (49.5/30/20/0.5 wt. %) (C1)

#84805 - $15.00 USD Received 6 Jul 2007; revised 22 Aug 2007; accepted 22 Aug 2007; published 28 Aug 2007

and PVK/7-DCST/ECZ/BBP/C60 (49.5/35/10/5/0.5 wt. %) (C2). Samples were prepared by laminating 105μm thick layers between glass slides with indium tin oxide (ITO) electrodes. The absorption coefficients/refractive indices of C1 and C2 at 633nm were measured to be 38 cm^{-1}/1.664 as 43 cm^{-1}/1.668, respectively.

The performance of a PR material is generally determined by measuring its diffraction efficiency, in degenerate four-wave mixing (DFWM) experiments illustrated in Fig. 1. Unlike transmission geometry, the writing beams are incident on opposite sides of the recording sample. In our configuration, each 633nm writing beam had an angle of $\theta_{1,2} = 72^0$ in air relative to the sample normal. The writing beams were *s*-polarized and had equal fluence (0.5 W/cm^2 each). A weak counter-propagating *p*-polarized beam probed the efficiency of the grating. The primary diffracted order was on the same side as the readout beam. The sample was slightly tilted (< 2^0) to separate the diffracted beam from the specular reflection off of the glass surface.

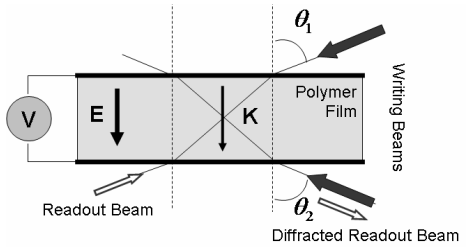

Fig. 1. Schematic of reflection geometry used in DFWM experiments. In the standard symmetric reflection geometry $\theta_1 = \theta_2$ is 72°, and $\varphi = 0$.

With this geometry, the external bias field has full projection on the grating vector for the creation of the space charge field. On the other hand due to the symmetry class of poled polymers, the effective electro-optic coefficient will decrease if the writing beam angles are reduced with respect to the sample normal. In our symmetric reflection geometry, the grating spacing is calculated to be 0.235μm at a wavelength of 633nm and zero degree slant angle. Notice that in this geometry the grating spacing is one order of magnitude less than in the case of the slanted transmission geometry. For such a short grating spacing, very large trap densities are required to create significant space-charge fields [16]. Most conventional PR polymers fail in this respect. Thus, the resulting refractive index changes in the reflection geometry tend to be small. In order to get high efficiencies in the reflection geometry, the effective number of trapping sites has to be increased. The peak diffraction efficiency is dependent on the effective trap density as well as on the first and second order nonlinearity contributions from chromophores. The density of trapping sites can be improved by selecting composite elements with appropriate energy levels to trap holes.

3. Results and discussion

At Bragg-matched incidence, the expression for the diffraction efficiency η in reflection can be simplified into the functional form:

$$\eta = \tanh^2\left[\frac{\pi \Delta n d}{\lambda\sqrt{\cos\alpha_1 \cos\alpha_2}}\hat{e}_i.\hat{e}_d\right]; \quad (1)$$

where Δn is the refractive index modulation amplitude of the phase grating, $\hat{e}_i$ and $\hat{e}_d$ are the unit polarization vectors of the incident reading beam and the diffracted beam, d is the thickness of the material, α_1 and α_2 are internal angles for the probe and diffracted beams. This function defines internal (lossless) diffraction efficiency in our polymers. The absorption and reflection losses are added later for calculation of the external diffraction efficiency.

#84805 - $15.00 USD Received 6 Jul 2007; revised 22 Aug 2007; accepted 22 Aug 2007; published 28 Aug 2007

Figure 2 presents the measurement of the diffraction efficiency in the DFWM geometry as a function of external field under steady-state conditions (1 second of illumination). Instead of observing the usual $\tanh^2(C\Delta n)$ dependence (where *C* is a constant) as predicted by (1), the diffraction efficiency reached a maximum followed by a subsequent decrease as the applied field was increased. When a slight offset (θ_0) was added to the readout angle, the diffraction efficiency peaked at different field magnitudes depending on the offset. For composition C1 with an external field of 85V/μm, the diffraction efficiency has exceeded 30% with a slight offset of reading angle from its initial near counter-propagating angle (1.7^0). Similarly, for composition C2, an internal diffraction efficiency of more than 60% has been observed at an offset angle of 1^0. On the other hand, in the case of s-polarized readout (not shown), the curve followed a typical $\tanh^2(C.\Delta n)$ pattern, right at Bragg angle without any additional offset angles. However the diffraction efficiency was low.

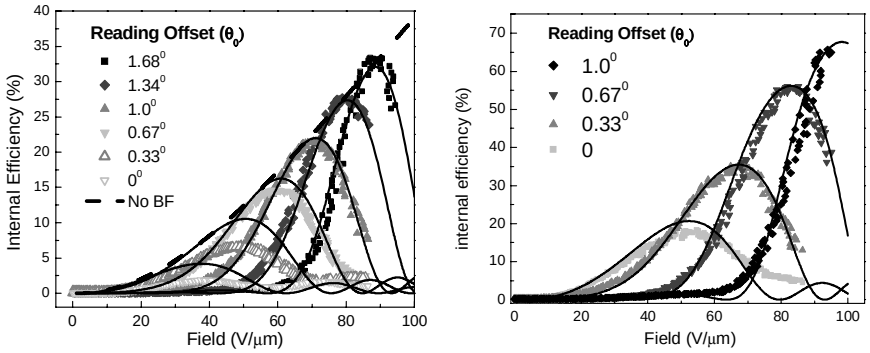

Fig. 2. Variation of diffraction efficiency with respect to the magnitude of electric field for a set of readout (p-polarized) offset angles in case of composition C1 (first graph) and C2 (second graph) including the fits to the Kogelnik theory. As the offset angle is varied, the diffraction efficiency peaks at different field magnitudes. The dashed line in first graph is a calculation for the case with no birefringence.

The PR nature of the hologram was confirmed through two-beam coupling measurements. For equal intensity writing beams, the net gain, Γ was more than 80 cm-1 at 76 V/μm for composition C1.

The traps in the C1 composite are believed to be due to conformational disorder in the PATPD polymer itself. The highest occupied molecular orbital (HOMO) energy levels for other elements (DBDC, ECZ and C60) in the system are below that of the hole-transporting matrix (PATPD). This material approach provides faster dynamics and longer operational stability [17]. However, the trap density is rather low as is the obtained diffraction efficiency in reflection geometry where short grating spacings are common. Therefore, we have followed a second composite approach based on PVK polymer (C2) and added other functional elements with similar HOMO energies to improve the density of traps in the system. The higher diffraction efficiency observed in composition C2 is believed to be due to the larger number of traps in the composite.

The dynamics of the index modulation can be extracted from a bi-exponential fit [8] that is correlated with the growth of the space charge field. At an applied field of 76 V/μm, the fast time constant for the build-up of the space-charge field was 14 ms and the slow time constant was 190 ms (C1). In an earlier publication [17], the dynamics of a device with the same composition measured in transmission geometry had similar time constants for the onset of diffraction. The fast time constant for composition C2 was ~80 ms.

The angular selectivity of the PR grating depends on various conditions, such as sample thickness, incident angle of the writing beams, refractive index of the material and grating spacing. To a first approximation, the Kogelnik theory predicts an angular half power

#84805 - $15.00 USD Received 6 Jul 2007; revised 22 Aug 2007; accepted 22 Aug 2007; published 28 Aug 2007

bandwidth given by $\Delta\theta_{1/2} \approx \Lambda / 2d$. The thicker the sample or the shorter the grating spacing, the greater the angular selectivity. For a fixed sample thickness, the PR grating is more sensitive to angular mismatch in reflection geometry than in transmission geometry. A small variation of the refractive index results in an altered readout angle according to Snell's law and in a variation in the propagation vectors of the writing beams. When the incident readout beam deviates from the Bragg angle, the diffraction efficiency inevitably decreases. Therefore, one should also take into account the Bragg mismatch due to the refractive index change in the case of low-T_g polymers to describe the behavior of the diffraction efficiency with respect to the external field strength.

Fortunately, in the slanted transmission geometry, the diffraction efficiency for polymeric PR materials with 105 μm or less thickness is hardly affected by the Bragg mismatch due to chromophore orientation. Therefore, it has been ignored in much of the previous work. The decrease in diffraction efficiency caused by the Bragg mismatch becomes more severe for thicker samples (> 300 μm) and smaller grating spacings (< 1 μm) [18].

In low-T_g PR polymers, the poling of chromophores along the applied field causes a change in the refractive index. Based on the oriented gas model [20], the first-order change in refractive indices of a poled polymer will be quadratic with the field:

$$\Delta n_X^{(1)} = \Delta n_Y^{(1)} = -\frac{1}{2}\Delta n_Z^{(1)} \propto E_0^2; \tag{2}$$

where, $\Delta n_X^{(1)}$, $\Delta n_Y^{(1)}$, $\Delta n_Z^{(1)}$ are the first-order index changes along each coordinate axis. The field is applied along the Z axis. A p-polarized readout beam will sense an increasing refractive index with a quadratic field dependence ($\Delta n_{BF}(E_0) = C_0 E_0^2$), where C_0 can be an experimental constant. Therefore, the internal angle for the readout beam will vary slightly with the magnitude of the external field. This can alter the Bragg condition if the grating spacing is small.

The variation in the internal readout angle due to poling can be expressed as (using Snell's Law):

$$\Delta\alpha(E_0, \alpha_0) = \frac{-\tan(\alpha_1)}{n} C_0 E_0^2 + \alpha_0; \tag{3}$$

where α_1 is the internal reading beam angle, C_0 is a constant for refractive index modulation due to birefringence, and α_0 is the offset angle inside the material set at the beginning of each measurement. The diffraction efficiency of a sample can be properly measured only when the incident angle of the reading beam satisfies the Bragg condition. In Figure 2, the decrease in diffraction efficiency is believed to be caused by Bragg mismatch due to the variation of refractive index with applied field.

Based on Kogelnik's coupled-wave theory [20], the equations describing the diffraction efficiency in the case of Bragg-mismatch can be modified as follows:

Obliquity factors:

$$\begin{aligned} c_i(E_0, \alpha_0) &= \cos\left[\alpha_1 + \Delta\alpha(E_0, \alpha_0)\right] \\ c_d(E_0, \alpha_0) &= \cos\left[\alpha_1 + \Delta\alpha(E_0, \alpha_0)\right] - \frac{\lambda}{\left[n + \Delta n_{BF}(E_0)\right]\Lambda}\cos\varphi \end{aligned} \tag{4}$$

Other factors:

$$\begin{aligned} \nu &= \frac{i\pi\Delta n d}{\lambda\sqrt{c_i c_d}}\hat{e}_i.\hat{e}_d \\ \xi &= \Delta\alpha K d\sin(\varphi - \alpha_1)/2c_d \end{aligned} \tag{5}$$

Diffraction efficiency:

#84805 - $15.00 USD Received 6 Jul 2007; revised 22 Aug 2007; accepted 22 Aug 2007; published 28 Aug 2007

$$\eta = 1/\left[1+\left(1-\xi^2/\nu^2\right)/\sinh^2\left(\sqrt{\nu^2-\xi^2}\right)\right] \tag{6}$$

where $\Delta\alpha$ is the deviation of the reading beam from the Bragg angle, α_1 is the Bragg matched angle for the readout beam which is same as the counter-propagating angle, Λ is the grating spacing, φ is the slant angle for the grating vector inside the sample, K is the magnitude of the grating vector, and d is the thickness of the material. Note that the major contribution to Bragg mismatch is due to an altered readout angle according to Snell's law. The contribution due to the variation in propagation vectors of the writing beams is very small.

The form of the diffraction efficiency curve has to be a superposition of its usual $\tanh^2$ behavior and the Bragg mismatch due to the variation of birefringence. The overall effect can be numerically calculated and the best fit for composition C1 can be obtained as given in Fig. 2. A relatively good fit can be obtained for the quadratic birefringence constant, C_0 with a value of *1.8e-18* [m^2/V^2] at offset angles close to the experimental values. In the case of composition C2, the C_0 value was calculated to be smaller (*~1.4e-18* [m^2/V^2]). The PVK based composite (C2) has less birefringence; therefore a slight offset in the readout angle pushes the peak of the efficiency to high bias fields. According to fits to the Kogelnik theory, we found a grating index modulation of 0.0025 for the PATPD composite, and 0.0048 for the PVK composite at 80V/μm. This analysis describes well the qualitative behavior of the diffraction efficiency curve with respect to increasing electric field, but does not describe exactly all aspects of the measurements. For low offset angles, the calculated values do not fully match with the experimental values. It is also necessary to take into account the experimental accuracy of the small angles used during the measurement. The internal angular bandwidth has been measured to be around 0.3° close to the Kogelnik approximated value of 0.27° given by $\Delta\theta_{1/2} \approx \Lambda/2d$.

We also measured the birefringence of these two composites through transmission ellipsometry experiments and the obtained values further support our numerical calculation shown above. The birefringence of a PR material can be experimentally characterized by measurements of the transmittance of the readout beam through a crossed polarizer analyzer arrangement. The transmittance of the readout beam is described by

$$I(E_0) = \sin^2\left[\frac{\pi\Delta n_{BF}(E_0)d}{\lambda\cos(\alpha)}\right]; \tag{7}$$

where α is the probe beam angle in the material and d is the thickness of the device. The variation of the birefringence of the PR polymer with electric field was determined when the external tilt angle of the sample was 72°. The measured result was fit to the theoretical transmittance function in (7) and the quadratic birefringence determined based on the oriented gas model. As shown in Fig. 3, the transmittance values are in a good agreement with a quadratic refractive index modulation. Composition C1 revealed more field-induced birefringence compared to C2. C_0 values calculated from these fits were *0.8e-18* [m^2/V^2] for C1, and *0.6e-18* [m^2/V^2] for C2. These birefringence constants are correlated with the values obtained from the fitting curves in DFWM experiments above. Due to the different nature of DFWM and ellipsometry measurements, agreement between the absolute values for the birefringence constants is not expected in these experiments.

#84805 - $15.00 USD Received 6 Jul 2007; revised 22 Aug 2007; accepted 22 Aug 2007; published 28 Aug 2007

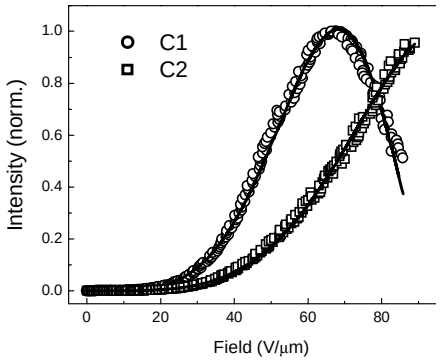

Fig. 3. The intensity readings from a transmission ellipsometry measurement for composition C1 (circles) and composition C2 (squares). The lines are fits based on Eq. (7). Notice that the C1 composition has a larger birefringence than the C2 composition, therefore the Bragg mismatch effect due to poling is more pronounced in DFWM experiments.

4. Conclusion

In summary, we have demonstrated significantly high diffraction efficiency (more than 60%) in a reflection geometry when we recorded gratings in low T_g photorefractive polymers. The reflection geometry has the practical advantage of having the reconstructing light on the same side as the viewer. In addition to that, a white light source can be used for reconstruction, unlike in the case of transmission geometry. In this geometry, the projection of applied bias field on the grating vector will also be large. However, volume holograms recorded in the reflection geometry are more sensitive to the reading angle and slight variations in the refractive index (such as those induced by poling of the chromophores) can easily lead to Bragg mismatch. The Bragg-matched reconstruction angle was observed to vary with the magnitude of the external applied field. This effect leads to modifications to the conventional diffraction efficiency relationship adding another degree of freedom for the effect of Bragg mismatch.

Acknowledgments

The authors acknowledge support from a U.S. Air Force Office of Scientific Research grant, the State of Arizona Technology and Research Initiative fund and an NSF-STC Materials and Devices for Information Technology Research grant. M. Eralp's email address is muhsin@optics.arizona.edu.

#84805 - $15.00 USD Received 6 Jul 2007; revised 22 Aug 2007; accepted 22 Aug 2007; published 28 Aug 2007